Timelike Holographic Complexity

Mohsen Alishahiha
School of Quantum Physics and Matter
Institute for Research in Fundamental Sciences (IPM),
P.O. Box 19395-5531, Tehran, Iran

Motivated by the pseudo-entropy program, we investigate timelike subregion complexity within the holographic "Complexity=Volume" framework, extending the usual spatial constructions to Lorentzian boundary intervals. For hyperbolic timelike regions in AdS geometries, we compute the corresponding bulk volumes and demonstrate that, despite the Lorentzian embedding, the resulting subregion complexity remains purely real. We further generalize our analysis to AdS black brane geometries, where the extremal surfaces can either be constant-time hypersurfaces or penetrate the horizon. In all cases, the computed complexity exhibits the same universal UV divergences as in the spacelike case but shows no imaginary contribution, underscoring its causal and geometric origin. This stands in sharp contrast with the complex-valued pseudo-entropy and suggests that holographic complexity preserves a genuinely geometric and real character even under Lorentzian continuation.

I. INTRODUCTION

Quantum entanglement has long been recognized as a fundamental probe of quantum correlations and spacetime structure in holographic theories [1–3]. Traditionally, entanglement entropy is defined for spatial subregions at a fixed time slice, capturing the pattern of quantum correlations among spatially separated degrees of freedom in the boundary theory. However, recent developments have extended this concept beyond equal-time slices, leading to a novel quantity known as pseudo-entropy [4–6]. This extension enables the study of entanglement-like measures for timelike subregions and for transitions between quantum states.

Pseudo-entropy generalizes entanglement entropy to the case of nontrivial quantum state transitions. Given an initial and a final state, $|\psi_i\rangle$ and $|\psi_f\rangle$, one defines a transition matrix

$$\tau = \frac{|\psi_f\rangle\langle\psi_i|}{\langle\psi_i|\psi_f\rangle}, \tag{1}$$

and the pseudo-entropy of a subsystem A (of a bipartite system $A \cup B$) as

$$S_A^{\text{pseudo}} = -\mathrm{Tr}\,\tau_A \log \tau_A, \qquad \tau_A = \mathrm{Tr}_B\,\tau. \tag{2}$$

Unlike conventional entanglement entropy, pseudo-entropy can acquire complex values due to the non-Hermitian nature of τ. Its real part quantifies a generalized correlation between $|\psi_i\rangle$ and $|\psi_f\rangle$, while its imaginary part encodes a phase-like structure associated with temporal or causal transitions. The appearance of such complex contributions points toward a richer analytic structure underlying holographic information measures.

In the context of AdS/CFT correspondence [7], pseudo-entropy naturally motivates the study of timelike extremal surfaces anchored on timelike boundary intervals [8–10]. These surfaces extend the Ryu–Takayanagi (RT) construction [1, 2] into Lorentzian regions of AdS, where the induced metric on the extremal surface may change signature. Such generalizations have attracted increasing interest in recent years (see *e.g.* [11–22]). The corresponding holographic entanglement entropy for timelike subregions generally acquires an imaginary part, which is interpreted as the bulk dual of the complex-valued pseudo-entropy. This complexification hints that other quantum information measures, such as quantum complexity, might also admit timelike or complexified extensions.

Holographic quantum complexity provides a geometric measure of how difficult it is to prepare a particular boundary state from a simple reference state using a minimal set of quantum operations. The two best-known proposals are the "Complexity=Volume" (CV) conjecture [23, 24]—further extended to subregion complexity in [25] (see also [26, 27])—and the "Complexity=Action" (CA) conjecture [28, 29], whose subregion version has been explored in [30–32]. These frameworks have deepened our understanding of information storage and state preparation in holographic field theories, particularly for spatially defined subsystems and global states.

Despite this progress, the generalization of holographic complexity to timelike subregions has remained largely unexplored. Motivated by the pseudo-entropy framework, we introduce and analyze a timelike version of subregion complexity within the CV proposal. This involves evaluating the bulk volume enclosed by timelike extremal surfaces—extending the original construction of [25] into Lorentzian regions of AdS. Conceptually, this provides a natural holographic dual for a measure of "temporal circuit depth" or the complexity associated with time evolution between quantum configurations in the boundary theory.

In this work, we focus first on timelike hyperbolic subregions in AdS_{d+2}, building on the explicit extremal surfaces found in [8, 9]. We compute the corresponding bulk volumes and analyze their divergence structures. Remarkably, we find that—unlike the case of pseudo-entropy—timelike subregion complexity remains purely real. This indicates that holographic complexity retains a purely geometric interpretation, even in the presence of Lorentzian embeddings, and may therefore probe aspects of spacetime geometry inaccessible to entanglement-based measures.

We then extend our analysis to thermal states described by AdS black brane geometries, where the presence of horizons renders the extremal surfaces more intricate. We show that, depending on the causal nature of the subregion, the extremal surfaces can penetrate the horizon, and the resulting complexity exhibits both universal UV divergences and finite, horizon-dependent corrections.

The remainder of this letter is organized as follows. In Sec. II, we compute the timelike subregion complexity for hyperbolic regions in pure AdS. In Sec. III, we generalize the construction to AdS black hole backgrounds and analyze the resulting behavior near and beyond the horizon. Sec. IV is devoted to concluding remarks and possible extensions.

II. TIMELIKE SUBREGION AND HOLOGRAPHIC VOLUME

Following [8, 9], we consider a timelike boundary subregion embedded in an AdS_{d+2} spacetime with $d \geq 1$. The bulk geometry is described by the metric

$$ds^2 = \frac{R^2}{r^2}\left(dr^2 + dy^2 - d\xi^2 + \xi^2 dX_{d-1}^2\right), \tag{3}$$

where y is a fixed spectator coordinate, X_{d-1} denotes the $(d-1)$-dimensional transverse space, and R is the AdS radius. The boundary subsystem is chosen as a timelike hyperbolic region $\xi^2 \leq \frac{T^2}{4}$, with T the boundary time interval. The corresponding area functional takes the form

$$A = H_{d-1} R^d \int dr\, \frac{\xi^{d-1}\sqrt{1-\xi'^2}}{r^d}, \tag{4}$$

where $H_{d-1} = \mathrm{Vol}(X_{d-1})$ is the transverse volume. Extremizing this functional yields two branches of extremal surfaces [8, 9]

$$\xi^2 = r^2 + \frac{T^2}{4}, \qquad \xi^2 = r^2 - \frac{T^2}{4}, \tag{5}$$

corresponding to spacelike and timelike surfaces, respectively. The timelike branch exists only for $r \geq \frac{T}{2}$, defining a causal cutoff in the bulk geometry.

These two branches together constitute the full extremal surface configuration that defines the timelike subregion problem. As demonstrated in [8, 9], while the area of the spacelike branch remains real, the timelike branch introduces an imaginary contribution to the entanglement entropy. This motivates studying its analog in holographic complexity, where one expects both real and potentially complex geometric contributions.

In the subregion complexity CV prescription [25], holographic complexity is proportional to the bulk volume enclosed by the extremal surfaces:

$$V = H_{d-1} R^{d+1} \int_{\xi \leq f(r)} dr\, d\xi\, \frac{\xi^{d-1}}{r^{d+1}}, \tag{6}$$

where $f(r)$ is the extremal profile defined in Eq. (5). In this case, the relevant volume is the region enclosed between the two branches, as illustrated in Figure 1. Performing the ξ integration then yields the volume difference between the branches, given by

$$V = \frac{2H_{d-1}R^{d+1}}{d}\left[\int_\epsilon^\infty dr \frac{(r^2+\frac{T^2}{4})^{\frac{d}{2}}}{r^{d+1}} - \int_{\frac{T}{2}}^\infty dr \frac{(r^2-\frac{T^2}{4})^{\frac{d}{2}}}{r^{d+1}}\right], \tag{7}$$

where ϵ is a UV cutoff near the boundary $r = 0$. The second integral starts at $r = T/2$ since the timelike branch exists only for $r \geq T/2$. The factor of 2 arises from the symmetry of the volume under consideration.

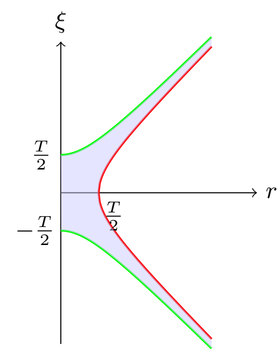

Figure 1. The colored region between the spacelike (green) and timelike (red) extremal surfaces represents the bulk volume associated with the timelike subregion complexity.

Following [25], the timelike subregion complexity is defined as

$$\mathcal{C}_{\mathrm{T}} = \frac{V}{GR}, \tag{8}$$

where G is the $(d+1)$-dimensional Newton constant. It is clear from Eq. (7) that both integrals individually exhibit IR divergences at $r \to \infty$, but these cancel in the difference, leaving a finite volume. The UV divergences at $r \to 0$ are regularized by ϵ.

Although Eq. (7) can be expressed in terms of hypergeometric functions for general d, it is more instructive to present explicit results for lower dimensions. Evaluating the integrals for $d = 1, 2, 3, 4$ gives

$$\text{AdS}_3: \quad \mathcal{C}_\text{T} = \frac{R}{G}\frac{T}{2\epsilon}, \tag{9}$$

$$\text{AdS}_4: \quad \mathcal{C}_\text{T} = \frac{V_1 R^2}{2G}\left(\frac{T^2}{8\epsilon^2} + \log\frac{T}{2\epsilon} + \frac{1}{2}\right), \tag{10}$$

$$\text{AdS}_5: \quad \mathcal{C}_\text{T} = \frac{V_2 R^3}{3G}\left(\frac{T^3}{24\epsilon^3} + \frac{3T}{4\epsilon}\right), \tag{11}$$

$$\text{AdS}_6: \quad \mathcal{C}_\text{T} = \frac{V_3 R^4}{4G}\left(\frac{T^4}{64\epsilon^4} + \frac{T^2}{4\epsilon^2} + \log\frac{T}{2\epsilon} + \frac{3}{4}\right). \tag{12}$$

The divergence structure mirrors that of the spacelike CV proposal: power-law UV divergences corresponding to short-distance correlations, and universal logarithmic terms appearing in even dimensions. The leading divergence scales with the volume of the boundary subregion, confirming that the dominant contribution to holographic complexity arises from the near-boundary geometry.

An important distinction emerges when comparing with the entanglement entropy of timelike regions: the complexity expressions in Eq. (9) are purely real. While the timelike branch of the extremal surface leads to an imaginary contribution in entanglement entropy due to the analytic continuation across the light cone, in the complexity–volume relation the integration is performed over a strictly Lorentzian region with $r \geq T/2$, yielding a real-valued geometric volume.

To gain a better intuition for the quantity we are computing, let us focus on the three-dimensional case. The corresponding extremal surfaces in Poincaré and global coordinates are depicted in Fig. 2 (see also [8]). In the context of entanglement entropy, when one transitions to global coordinates, the timelike branch becomes apparent, giving rise to the imaginary contribution in the pseudo-entropy. For complexity, if one ignores the timelike surface, the relevant bulk volume would appear to be that enclosed by the spacelike RT curve and the Poincaré horizon in the global coordinate patch. However, once the timelike extremal surface is included, the proper volume is the region enclosed between the spacelike and timelike branches—illustrated by the shaded region in Fig. 2.

One might naturally wonder whether this configuration implies a hidden causal connection between the two branches, absent in the usual spacelike case, which could in principle lead to an imaginary contribution to the complexity. At present, however, it remains unclear whether such a causal volume genuinely exists [1].

From a technical perspective, for odd d both limits of the timelike integral acquire phase factors that cancel, leaving a purely real result. Hence, timelike complexity measures only the accessible Lorentzian bulk volume, while pseudo-entropy captures phase information related to temporal correlations.

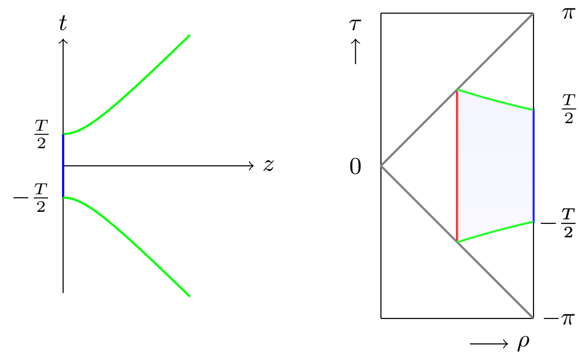

Figure 2. Extremal surfaces for a timelike entangling region (blue interval) in Poincaré (left) and global (right) coordinates. In the global case, in addition to the spacelike extremal surface (green), there exists a timelike one (red). The timelike subregion complexity corresponds to the bulk volume enclosed between these two surfaces, illustrated by the shaded (colored) region. This figure essentially reproduces Fig. 3 of [8] for clarity and comparison. Here, (r, z) and (τ, ρ) denote the Poincaré and global coordinate systems, respectively.

Comparing our results with those for spacelike subregions obtained in [25], we find that although the overall divergence structure of timelike subregion complexity closely parallels the spacelike case, the two are not related by a simple Wick rotation. Both share the same hierarchy of UV divergences—power-law terms reflecting short-distance correlations and logarithmic terms in even dimensions—but their finite parts differ in both magnitude and interpretation. In particular, for odd-dimensional AdS backgrounds, timelike complexity lacks the universal constant term that characterizes its spacelike counterpart. This absence suggests that timelike complexity has a fundamentally distinct geometric origin, one not obtainable by analytic continuation of the spatial result. Rather, it arises directly from the Lorentzian causal structure of the extremal hypersurface.

To further clarify this point, consider repeating the extremization procedure for a spacelike subregion possessing spherical symmetry at the boundary. The corresponding area functional admits two distinct extremal solutions:

$$\xi(r) = \sqrt{\ell^2 - r^2}, \qquad \xi(r) = i\sqrt{\ell^2 + r^2}, \tag{13}$$

where ℓ is the radius of the boundary entangling region.

The first branch corresponds to the well-known RT surface [1], which provides the minimal-area prescription for holographic entanglement entropy and forms the basis for computing holographic subregion complexity [25]. The second branch, however, is purely imaginary and has traditionally been excluded because it does not correspond to a real Lorentzian extremal surface in the AdS bulk. In the usual treatment, this complex embedding is interpreted as unphysical, as it extends beyond the domain of

[1] I would like thank T. Takayanagi for a comment on this point.

real-valued minimal surfaces anchored on the boundary.

From the present perspective, however, this "discarded" branch carries deep physical significance. Upon analytic continuation, it reproduces the timelike extremal branch encountered in the study of timelike entanglement entropy and timelike subregion complexity. The imaginary embedding coordinate $\xi = i\sqrt{\ell^2 + r^2}$ corresponds to a continuation of the minimal surface across the light cone, thereby encoding the causal extension of the entangling region into the timelike domain. Its contribution is responsible for the appearance of the imaginary component in pseudo-entropy, reflecting phase information associated with non-unitary or time-reflected evolutions of the boundary state.

In this sense, the two branches—one real and one imaginary—are not independent but rather analytic continuations of a unified geometric configuration. The real branch represents the standard RT surface probing spatial entanglement, while the imaginary branch extends the geometry into a "shadow" region of AdS, corresponding to the temporal or causally continued part of the boundary subregion. This complexified structure naturally bridges spacelike and timelike holographic quantities: the real branch encodes spatial correlations, whereas the imaginary branch captures the causal and temporal entanglement information underlying pseudo-entropy.

Within the framework of holographic complexity for spacelike subregions, only the real Lorentzian volume contributes directly to the CV proposal, providing a real-valued geometric measure of computational depth. However, the presence of an imaginary extremal branch suggests that a more general, complexified notion of holographic complexity may exist—one that unifies spatial and temporal information within a single analytic structure. Such an extension could naturally connect holographic complexity, pseudo-entropy, and causal holographic information through complex AdS embeddings, offering a richer picture of quantum information geometry in Lorentzian spacetimes. Nonetheless, as our explicit calculations show, even for the timelike subsystem—where the extremal configuration includes a timelike branch—the resulting complexity remains entirely real, reflecting the geometric rather than entropic nature of the CV prescription.

III. TIMELIKE SUBREGION COMPLEXITY FOR ADS BLACK HOLES

It is natural to extend our discussion of timelike subregion complexity to thermal states, which are holographically dual to AdS black hole or black brane geometries. In this context, the thermal nature of the boundary state is encoded in the presence of a horizon, introducing a new geometric scale that influences the causal structure of the extremal surfaces. For concreteness, we consider a $(d{+}2)$-dimensional AdS black hole with metric

$$ds^2 = \frac{R^2}{r^2}\left(-f(r)\,dt^2 + \frac{dr^2}{f(r)} + dx^2 + dY_{d-1}^2\right), \quad (14)$$

where

$$f(r) = 1 - \frac{r^{d+1}}{r_h^{d+1}}, \quad (15)$$

and r_h denotes the horizon radius. The conformal boundary lies at $r = 0$.

We consider a timelike subregion in the form of a strip extending along the y_i directions but bounded in time by the finite interval $t \in [-T/2, T/2]$ at fixed spatial coordinate x. Although, unlike the hyperbolic case discussed in the previous section, this setup lacks a clear interpretation of bulk extremal surface, we can still follow the general extremization procedure for the area functional associated with a timelike embedding $t = t(r)$ [9]. The induced metric on the hypersurface is

$$ds_{\text{ind}}^2 = \frac{R^2}{r^2}\left[\left(\frac{1}{f(r)} - f(r)\,t'(r)^2\right)dr^2 + dY_{d-1}^2\right], \quad (16)$$

where $t'(r) = dt/dr$ and dY_{d-1}^2 denotes the $(d-1)$-dimensional transverse section. The corresponding area functional is

$$A = \mathcal{R}_{d-1}R^d \int dr\, \frac{\sqrt{\frac{1}{f(r)} - f(r)\,t'(r)^2}}{r^d}, \quad (17)$$

with $\mathcal{R}_{d-1} = \mathrm{Vol}(Y_{d-1})$.

Extremizing this functional yields a conserved quantity,

$$\frac{-f(r)t'(r)}{r^d\sqrt{\frac{1}{f(r)} - f(r)t'(r)^2}} = \text{constant}, \quad (18)$$

which can be interpreted as an "energy" parameter for the surface profile $t(r)$. For real-valued $t'(r)$ this constant must be real; however, for timelike subregions this reality condition is subtle, and in general no globally real solution exists unless the extremal surface extends beyond the horizon.

Besides the trivial solution $t'(r) = 0$, the presence of a horizon allows for an extremal surface that penetrates it, with the turning point r_0 lying behind the horizon ($r_0 > r_h$). This possibility is not merely formal—it closely parallels the behavior of extremal surfaces in time-dependent backgrounds such as Vaidya geometries [33], where the surface crosses horizons to capture causal correlations. Even though our setup is static, the subregion itself is intrinsically time-dependent, which justifies such an extension. Under this assumption, the extremal surface satisfies

$$\frac{f(r)\,t'(r)}{\sqrt{\frac{1}{f(r)} - f(r)t'(r)^2}} = \sqrt{\tilde{f}(r_0)}\left(\frac{r}{r_0}\right)^d, \quad (19)$$

where

$$\tilde{f}(r_0) = \left(\frac{r_0}{r_h}\right)^{d+1} - 1, \tag{20}$$

for $r_0 > r_h$. Solving for $t'(r)$ gives

$$t'(r) = -\frac{\left(\frac{r}{r_0}\right)^d \sqrt{\tilde{f}(r_0)}}{f(r)\sqrt{f(r) + \left(\frac{r}{r_0}\right)^{2d} \tilde{f}(r_0)}}. \tag{21}$$

The CV-type volume enclosed by this extremal surface is

$$V = 2\,\mathcal{R}_{d-1} R^{d+1} \int dr\, \frac{t(r)}{r^{d+1}}, \tag{22}$$

where the factor of two reflects time-reflection symmetry. Integrating by parts and using $t(0) = T/2$, we obtain

$$\mathcal{C}_{\mathrm{T}} = \frac{\mathcal{R}_{d-1} R^d T}{dG\,\epsilon^d} + \frac{2\mathcal{R}_{d-1} R^d}{dG} \int_\epsilon^{r_0} dr\, \frac{t'(r)}{r^d}, \tag{23}$$

with ϵ a UV cutoff. Substituting (21) yields [2]

$$\mathcal{C}_{\mathrm{T}} = \frac{\mathcal{R}_{d-1} R^d T}{dG\,\epsilon^d} - \frac{2\mathcal{R}_{d-1} R^d \sqrt{\tilde{f}(r_0)}}{dG\, r_0^d} \int_\epsilon^{r_0} \frac{dr}{f(r)\sqrt{f(r) + \left(\frac{r}{r_0}\right)^{2d} \tilde{f}(r_0)}}. \tag{24}$$

The leading divergence is proportional to the boundary volume of the subsystem, as expected from the near-boundary AdS structure. Importantly, the total timelike complexity remains real, even when the extremal surface penetrates the horizon. This behavior contrasts with that of timelike entanglement entropy, which typically acquires imaginary contributions associated with pseudo-entropy.

Although we have so far ignored the trivial $t'(r) = 0$ configuration—corresponding to a constant-time slice extending from the boundary to the horizon—it is plausible that, under certain conditions, a transition could occur between this static branch and the horizon-penetrating one. Such a transition would resemble phase changes between distinct extremal surfaces in the usual entanglement entropy context.

It is worth noting that in [34, 35], the authors propose a systematic holographic prescription for timelike entanglement entropy in which the bulk geometry is essentially complexified, and one is led to consider complex extremal surfaces anchored on a timelike boundary strip. Remarkably, the horizon-penetrating solution we obtain in the Lorentzian setup coincides precisely with one of these complex extremal surfaces, providing a fully real-valued analogue in our construction while capturing the same underlying causal and geometric features[3].

IV. CONCLUSION

In this work, we have introduced and systematically analyzed the notion of timelike subregion complexity within the holographic CV framework. Motivated by the pseudo-entropy program, we have extended the study of holographic complexity from spatial to timelike boundary regions and evaluated the corresponding bulk volumes for both pure AdS and AdS black brane geometries.

For timelike hyperbolic regions in pure AdS_{d+2}, we showed that the bulk volume enclosed between the spacelike and timelike extremal surfaces remains purely real, despite the Lorentzian nature of the embedding. This stands in sharp contrast with the case of pseudo-entropy, where analytic continuation across the light cone generically produces an imaginary component. The absence of any imaginary part in the complexity indicates that the CV functional retains a genuinely geometric interpretation even when extended to timelike configurations. In this sense, timelike complexity measures the accessible Lorentzian volume bounded by causally admissible surfaces, providing a probe of spacetime geometry that is insensitive to analytic continuation or phase structure.

We then extended our analysis to thermal states dual to AdS black branes, where the causal structure and the presence of a horizon introduce new subtleties. In this case, extremal surfaces can penetrate the horizon, depending on the causal character of the boundary subregion, while a trivial solution corresponding to a constant-time hypersurface also exists, extending smoothly from the boundary to the horizon. Remarkably, even when the extremal surface crosses the horizon, the resulting CV volume—and hence the subregion complexity—remains entirely real. This reinforces the interpretation of timelike complexity as a measure of accessible bulk volume determined by causal reach rather than analytic continuation. It is also plausible that a transition could occur between the trivial and horizon-penetrating branches, signaling a new type of geometric phase structure.

The absence of any imaginary contribution in $\mathcal{C}_{\mathrm{T}}$ suggests that holographic complexity possesses a fundamentally different analytic structure from that of

[2] Technically, evaluating this integral is subtle because the integration range necessarily crosses the horizon, where the factor $f(r)$ vanishes and may appear to cause divergences. However, by carefully splitting the integration domain into two regions—$[\epsilon, r_h]$ and $[r_h, r_0]$ —and performing the integration on each side separately, one finds that the potentially divergent contributions from both sides of the horizon cancel, yielding a finite and smooth result across the horizon.

[3] I would like to thank M. Heller for bringing these insightful papers to my attention.

pseudo-entropy. Whereas pseudo-entropy can reflect features of transition amplitudes—such as phase information—complexity appears to probe the underlying geometry of information itself. Its purely real character indicates that holographic complexity encodes the intrinsic "depth" or cost of traversing the bulk spacetime, independent of any temporal analytic continuation.

This purely real nature is, in fact, not unexpected. Although the construction originates from the transition matrix (1), which is not Hermitian, it remains a well-posed and meaningful question to ask how "distant" the final state $|\psi_f\rangle$ is from the initial state $|\psi_i\rangle$. In this sense, $\mathcal{C}_{\mathrm{T}}$ can be interpreted as quantifying the minimal number of effective "gates" or operations required to transform $|\psi_i\rangle$ into $|\psi_f\rangle$ restricted to a subregion—a quantity that is naturally real.

Of course, an important open question remains—namely, how to compute timelike complexity directly from the boundary field theory. Even for spatial subregions, a precise field-theoretic definition of subregion complexity is still lacking, with partial insights coming from circuit complexity, path-integral optimization, or tensor-network approaches. Extending these frameworks to Lorentzian or timelike subregions poses additional conceptual and technical challenges, as one must incorporate causal and non-unitary aspects of boundary dynamics. A consistent field-theoretic formulation of timelike complexity would thus not only clarify the operational meaning of our holographic construction but also reveal how temporal and causal structures are encoded in the boundary state space.

We note also that working with timelike entangling regions reveals an intriguing new feature. By relaxing the physical boundary conditions on the entangling region, additional extremal surfaces can emerge, though their physical interpretation remains uncertain. In particular, we could identify a Lorentzian branch with an induced metric of Lorentzian signature, corresponding to an extremal surface that originates from a point in the bulk and terminates at the horizon. Such configurations suffer from infrared divergences, which typically arise from the near-horizon region of the geometry where the redshift factor becomes large. In this regime, the integrand of the corresponding volume or area functional develops a logarithmic divergence, signaling that the extremal surface probes deep into the infrared part of the bulk spacetime. Physically, this behavior reflects the accumulation of contributions from regions close to the horizon, where the proper volume effectively becomes infinite due to the warping of the metric. Understanding the precise regularization and physical interpretation of these IR divergences—whether they correspond to long-time or large-scale phenomena in the dual field theory—remains an open and interesting question.

Very recently, the paper [36] (see also [37]) appeared, in which the authors investigated the dynamics of spatial subregion complexity under time evolution and uncovered a series of striking behaviors. They showed that for subsystems larger than half the total system, the complexity grows linearly for exponentially long times, whereas for smaller subsystems the growth halts and eventually reverses, leading to a sharp transition at the half-size threshold. At finite temperature, additional critical subsystem sizes emerge, determining whether the complexity saturates instantaneously or continues to grow.

Although their setup focuses on spatial subregions evolving in time, it shares deep conceptual parallels with our Lorentzian analysis. Both frameworks reveal that subregion complexity is highly sensitive to causal structure and the presence of horizons or effective causal barriers. In particular, the sharp transitions identified in [36] may correspond, in our timelike setup, to transitions between distinct extremal branches—such as the constant-time and horizon-penetrating surfaces. Moreover, the finite-temperature critical behavior observed in their study closely parallels our finding that timelike extremal surfaces exhibit qualitatively different regimes depending on whether the turning point lies inside the horizon or corresponds to a static configuration, hinting at analogous transition phenomena in the timelike CV framework.

A natural extension of our work, beyond generalizations to other geometries, would be to formulate and compute the timelike version of the CA conjecture on a Wheeler–DeWitt patch anchored to a timelike interval (see [32] for primarily computations in this direction).

ACKNOWLEDGEMENTS

I would like to thank Andreas Karch, Souvik Banerjee and Tadashi Takayanagi for their valuable comments. I am also grateful to Kyriakos Papadodimas and Mohammad Javad Vasli for many insightful discussions on various aspects of holographic complexity. I would further like to thank the CERN Department of Theoretical Physics for their warm hospitality during the course of this work. This research was supported by the Iran National Science Foundation (INSF) under Project No. 4023620. I also acknowledge the assistance of ChatGPT for editorial help in refining and polishing the manuscript.

[1] S. Ryu and T. Takayanagi, "Holographic derivation of entanglement entropy from AdS/CFT," Phys. Rev. Lett. **96** (2006), 181602 doi:10.1103/PhysRevLett.96.181602 [arXiv:hep-th/0603001 [hep-th]].

[2] S. Ryu and T. Takayanagi, "Aspects of Holographic Entanglement Entropy," JHEP **08** (2006), 045 [arXiv:hep-th/0605073 [hep-th]].
[3] V. E. Hubeny, M. Rangamani and T. Takayanagi, "A Covariant holographic entanglement entropy proposal," JHEP **07** (2007), 062 [arXiv:0705.0016 [hep-th]].
[4] Y. Nakata, T. Takayanagi, Y. Taki, K. Tamaoka and Z. Wei, "New holographic generalization of entanglement entropy," Phys. Rev. D **103** (2021) no.2, 026005 [arXiv:2005.13801 [hep-th]].
[5] A. Mollabashi, N. Shiba, T. Takayanagi, K. Tamaoka and Z. Wei, "Pseudo Entropy in Free Quantum Field Theories," Phys. Rev. Lett. **126** (2021) no.8, 081601 [arXiv:2011.09648 [hep-th]].
[6] A. Mollabashi, N. Shiba, T. Takayanagi, K. Tamaoka and Z. Wei, "Aspects of pseudoentropy in field theories," Phys. Rev. Res. **3** (2021) no.3, 033254 [arXiv:2106.03118 [hep-th]].
[7] J. M. Maldacena, "The Large N limit of superconformal field theories and supergravity," Adv. Theor. Math. Phys. **2** (1998), 231-252 [arXiv:hep-th/9711200 [hep-th]].
[8] K. Doi, J. Harper, A. Mollabashi, T. Takayanagi and Y. Taki, "Pseudoentropy in dS/CFT and Timelike Entanglement Entropy," Phys. Rev. Lett. **130** (2023) no.3, 031601 [arXiv:2210.09457 [hep-th]].
[9] K. Doi, J. Harper, A. Mollabashi, T. Takayanagi and Y. Taki, "Timelike entanglement entropy," JHEP **05** (2023), 052 [arXiv:2302.11695 [hep-th]].
[10] K. Narayan, "de Sitter space, extremal surfaces, and time entanglement," Phys. Rev. D **107** (2023) no.12, 126004 doi:10.1103/PhysRevD.107.126004 [arXiv:2210.12963 [hep-th]].
[11] P. Wang, H. Wu and H. Yang, "Fix the dual geometries of $T\bar{T}$ deformed CFT_2 and highly excited states of CFT_2," Eur. Phys. J. C **80** (2020) no.12, 1117 [arXiv:1811.07758 [hep-th]].
[12] K. Narayan, "de Sitter future-past extremal surfaces and the entanglement wedge," Phys. Rev. D **101** (2020) no.8, 086014 doi:10.1103/PhysRevD.101.086014 [arXiv:2002.11950 [hep-th]].
[13] B. Liu, H. Chen and B. Lian, "Entanglement entropy of free fermions in timelike slices," Phys. Rev. B **110** (2024) no.14, 144306 [arXiv:2210.03134 [cond-mat.stat-mech]].
[14] Z. Li, Z. Q. Xiao and R. Q. Yang, "On holographic time-like entanglement entropy," JHEP **04** (2023), 004 [arXiv:2211.14883 [hep-th]].
[15] K. Narayan and H. K. Saini, "Notes on time entanglement and pseudo-entropy," Eur. Phys. J. C **84** (2024) no.5, 499 [arXiv:2303.01307 [hep-th]].
[16] K. Narayan, "Further remarks on de Sitter space, extremal surfaces, and time entanglement," Phys. Rev. D **109** (2024) no.8, 086009 [arXiv:2310.00320 [hep-th]].
[17] S. S. Jena and S. Mahapatra, "A note on the holographic time-like entanglement entropy in Lifshitz theory," JHEP **01** (2025), 055 [arXiv:2410.00384 [hep-th]].
[18] M. Afrasiar, J. K. Basak and D. Giataganas, "Holographic timelike entanglement entropy in non-relativistic theories," JHEP **05** (2025), 205 [arXiv:2411.18514 [hep-th]].
[19] C. Nunez and D. Roychowdhury, "Timelike entanglement entropy: A top-down approach," Phys. Rev. D **112** (2025) no.2, 026030 [arXiv:2505.20388 [hep-th]].
[20] Z. X. Zhao, L. Zhao and S. He, "Timelike Entanglement Entropy in Higher Curvature Gravity," [arXiv:2509.04181 [hep-th]].
[21] X. Jiang, H. Wu and H. Yang, "Timelike entanglement entropy Revisited," [arXiv:2503.19342 [hep-th]].
[22] V. Mohan and W. Sybesma, "De Sitter Complexity Grows Linearly in the Static Patch," [arXiv:2508.10093 [hep-th]].
[23] L. Susskind, "Computational Complexity and Black Hole Horizons," Fortsch. Phys. **64** (2016), 24-43 [arXiv:1403.5695 [hep-th]].
[24] D. Stanford and L. Susskind, "Complexity and Shock Wave Geometries," Phys. Rev. D **90** (2014) no.12, 126007 [arXiv:1406.2678 [hep-th]].
[25] M. Alishahiha, "Holographic Complexity," Phys. Rev. D **92** (2015) no.12, 126009 [arXiv:1509.06614 [hep-th]].
[26] O. Ben-Ami and D. Carmi, "On Volumes of Subregions in Holography and Complexity," JHEP **11** (2016), 129 [arXiv:1609.02514 [hep-th]].
[27] R. Abt, J. Erdmenger, H. Hinrichsen, C. M. Melby-Thompson, R. Meyer, C. Northe and I. A. Reyes, "Topological Complexity in $\mathrm{AdS}_3/\mathrm{CFT}_2$," Fortsch. Phys. **66** (2018) no.6, 1800034 [arXiv:1710.01327 [hep-th]].
[28] A. R. Brown, D. A. Roberts, L. Susskind, B. Swingle and Y. Zhao, Phys. Rev. Lett. **116** (2016) no.19, 191301 [arXiv:1509.07876 [hep-th]].
[29] A. R. Brown, D. A. Roberts, L. Susskind, B. Swingle and Y. Zhao, "Complexity, action, and black holes," Phys. Rev. D **93** (2016) no.8, 086006 [arXiv:1512.04993 [hep-th]].
[30] D. Carmi, R. C. Myers and P. Rath, "Comments on Holographic Complexity," JHEP **03** (2017), 118 [arXiv:1612.00433 [hep-th]].
[31] C. A. Agón, M. Headrick and B. Swingle, "Subsystem Complexity and Holography," JHEP **02** (2019), 145 doi:10.1007/JHEP02(2019)145 [arXiv:1804.01561 [hep-th]].
[32] M. Alishahiha, K. Babaei Velni and M. R. Mohammadi Mozaffar, "Black hole subregion action and complexity," Phys. Rev. D **99** (2019) no.12, 126016 doi:10.1103/PhysRevD.99.126016 [arXiv:1809.06031 [hep-th]].
[33] H. Liu and S. J. Suh, "Entanglement growth during thermalization in holographic systems," Phys. Rev. D **89** (2014) no.6, 066012 [arXiv:1311.1200 [hep-th]].
[34] M. P. Heller, F. Ori and A. Serantes, "Geometric Interpretation of Timelike Entanglement Entropy," Phys. Rev. Lett. **134** (2025) no.13, 131601 [arXiv:2408.15752 [hep-th]].
[35] M. P. Heller, F. Ori and A. Serantes, "Temporal Entanglement from Holographic Entanglement Entropy," [arXiv:2507.17847 [hep-th]].
[36] Y. Fan, N. Hunter-Jones, A. Karch and S. Mittal, "Sharp Transitions for Subsystem Complexity," [arXiv:2510.18832 [hep-th]].
[37] J. Haah and D. Stanford, "Growth and collapse of subsystem complexity under random unitary circuits," [arXiv:2510.18805 [quant-ph]].